NASA TECHNICAL NOTE

NASA TN D-6951

NASA TN D-6951

METEOROID IMPACTS ON MARS AND THE SECONDARY PARTICLE ENVIRONMENT

by Donald H. Humes and T. Dale Bess

Langley Research Center
Hampton, Va. 23365

NATIONAL AERONAUTICS AND SPACE ADMINISTRATION • WASHINGTON, D. C. • OCTOBER 1972

1. Report No.	2. Government Accession No.	3. Recipient's Catalog No.
NASA TN D-6951		

4. Title and Subtitle	5. Report Date
METEOROID IMPACTS ON MARS AND THE SECONDARY PARTICLE ENVIRONMENT	October 1972
	6. Performing Organization Code

7. Author(s)	8. Performing Organization Report No.
Donald H. Humes and T. Dale Bess	L-8479
	10. Work Unit No. 815-20-09-01
9. Performing Organization Name and Address	11. Contract or Grant No.
NASA Langley Research Center Hampton, Va. 23365	
	13. Type of Report and Period Covered
12. Sponsoring Agency Name and Address	Technical Note
National Aeronautics and Space Administration Washington, D.C. 20546	14. Sponsoring Agency Code

15. Supplementary Notes

16. Abstract

The degree to which the thin Martian atmosphere filters out meteoroids approaching the Martian surface was calculated by using a model of the meteoroid environment, a model of the Martian atmosphere, and equations of meteor physics. The secondary particle environment on the surface of Mars caused by the material ejected from meteoroid craters was modeled. The model consists of the mass distribution and the speed distribution of the secondary particles. Calculations were made of the penetration flux for aluminum structures on the Martian surface. The penetration hazard on the Martian surface was compared with the penetration hazard in space near Mars and on the lunar surface.

17. Key Words (Suggested by Author(s))	18. Distribution Statement
Mars Meteoroid impact Impact damage	Unclassified – Unlimited

19. Security Classif. (of this report)	20. Security Classif. (of this page)	21. No. of Pages	22. Price*
Unclassified	Unclassified	37	$3.00

*For sale by the National Technical Information Service, Springfield, Virginia 22151

METEOROID IMPACTS ON MARS AND THE SECONDARY PARTICLE ENVIRONMENT

By Donald H. Humes and T. Dale Bess
Langley Research Center

SUMMARY

The degree to which the thin Martian atmosphere filters out meteoroids approaching the Martian surface was calculated by using a model of the meteoroid environment, a model of the Martian atmosphere, and equations of meteor physics. The secondary particle environment on the surface of Mars caused by the material ejected from meteoroid craters was modeled. The model consists of the mass distribution and the speed distribution of the secondary particles. Calculations were made of the penetration flux for aluminum structures on the Martian surface. The penetration hazard on the Martian surface was compared with the penetration hazard in space near Mars and on the lunar surface.

INTRODUCTION

Although the Earth is cloaked with a heavy atmosphere which prevents impacts on the surface from all but the most massive meteoroids, the Moon is unprotected and its surface absorbs the energy of every meteoroid encounter. The material ejected from the craters presents a potential penetration hazard to spacecraft on the surface. This material also contributes to the formation of the lunar regolith. Meteoroid impacts on the Moon have been studied by many investigators. Dohnanyi used the size distribution of lunar craters to estimate the size distribution of meteoroids. (See ref. 1.) The flux and speed of the ejecta material have been calculated by Gault, Shoemaker, and Moore (ref. 2) and Zook (ref. 3). The depth of the lunar regolith at Tranquility Base was estimated by Shoemaker, Hait, Swann, Schleicher, Dahlem, Schaber, and Sutton (ref. 4) by using the distribution of crater size; the sizes of the craters range around a few meters in diameter.

Mars differs from the Moon in at least two respects that affect meteoroid impacts on the surface. Mars is nearer to the asteroid belt and should encounter more asteroidal meteoroids, and Mars has a thin atmosphere which should provide some protection for the surface. It is not obvious whether meteoroids have more of an effect on the Martian surface or on the lunar surface.

The purposes of this paper are (1) to determine the degree to which the Martian atmosphere protects the surface by filtering out meteoroids, (2) to estimate the flux and speed of secondary particles which are ejected from meteoroid craters on Mars, and (3) to compare the penetration hazard to a spacecraft on the Martian surface with the penetration hazard on the lunar surface and with the hazard in space near Mars.

No attempt is made to estimate the size distribution of craters on the Martian surface because Martian winds could quickly alter the surface features. Also no attempt was made to estimate the size distribution of the particles in the regolith because (1) the experimental data on the ejecta from craters in reference 2 were not well defined for small particles, less than 10 μm, because of the difficulty in capturing these small particles and (2) strong winds on Mars could cause erosion of the larger particles and have a large effect on the size distribution.

SYMBOLS

A	meteoroid shape factor (1.21)
a	mass-dependent variable in probability density function for speed of secondary particles, s/m
C_1	constant, 6.92×10^{11} kg-K$^{1/2}$/m^{2}s
C_2	heat capacity of meteoroid, 1×10^3 J/kg-K
C_3	constant, 5.78×10^4 K
E	kinetic energy of meteoroid, J
$f(V,\theta)$	residual mass function for meteoroids entering atmosphere with initial speed V and initial zenith angle θ
$G(V_e)$	fraction of total mass of ejecta from a single impact that has speed V_e or greater
g(V)	meteoroid speed probability density function
H	altitude of meteoroid above Martian surface, m

$h(\theta)$ meteoroid impact angle probability density function

k_1 constant, $10^{-4.9}$ s^2/m^2

L mean free path for atmospheric molecules, m

ℓ plate thickness, m

M_e total mass of all particles ejected from a meteoroid crater, kg

m mass of meteoroid, kg

m_b mass of largest ejecta particle from a single crater, kg

m_e mass of ejecta particle, kg

m_1 mass of meteoroid outer shell which is heated to temperature T, kg

m' cumulative mass of ejecta particles that have mass m_e or smaller, due to a single meteoroid impact, kg

$\overline{m}$ cumulative mass of ejecta particles that have speed V_e or greater, due to a single meteoroid impact, kg

$N_{V_{e1}-V_{e2}}$ number of ejecta particles with speeds in the range V_{e1} to V_{e2} ejected from a single crater

$p(\theta,V)$ penetration equation for a structure in terms of minimum mass required to penetrate the structure

Q heat of ablation of meteoroid, 1.36×10^6 J/kg

R radius of meteoroid, m

T absolute temperature of heated part of meteoroid, K

t time, s

V speed of meteoroid, m/s

V_e speed of ejecta particle, m/s

V_{e1}, V_{e2} particular speeds of ejecta particles, m/s

Γ drag coefficient, $1.068\left(\frac{L}{R}\right)^{0.15}$ (where $0.5 \leqq \Gamma \leqq 1$)

δ meteoroid mass density, kg/m^3

ϵ emissivity of meteoroid, 0.7

θ impact or entry angle of meteoroid measured from the normal to structure surface or atmosphere, rad

Λ heat-transfer coefficient, $\sqrt{1.6\,\frac{L}{R}}$ (where $0.1 \leqq \Lambda \leqq 1$)

ρ atmospheric density, kg/m^3

σ Stefan-Boltzmann constant, $5.67 \times 10^{-8}\ WK^4/m^2$

ϕ cumulative mass-flux of meteoroids, $m^{-2}s^{-1}$

ϕ_a cumulative mass-flux of asteroidal meteoroids, $m^{-2}s^{-1}$

ϕ_c cumulative mass-flux of cometary meteoroids, $m^{-2}s^{-1}$

ϕ_E cumulative energy flux of meteoroids, $m^{-2}s^{-1}$

ϕ_s cumulative mass-flux of secondary particles, $m^{-2}s^{-1}$

$\phi_{\frac{V_{e1}+V_{e2}}{2},m_e}$ flux of ejecta particles with speed $\frac{V_{e1}+V_{e2}}{2}$ and corresponding mass m_e which are ejected from all craters formed by meteoroids of a particular kinetic energy E, $m^{-2}s^{-1}$

ψ_p penetration flux for a structure, $m^{-2}s^{-1}$

APPROACH

The approach taken to determine the degree to which the thin Martian atmosphere protects the surface from meteoroid impact was first to determine the flux of meteoroids on the upper atmosphere of Mars by using the model of the interplanetary meteoroid environment in reference 5, and then to determine the flux of meteoroids on the Martian surface by calculating the losses caused by encountering the Martian atmosphere from the equations of meteor physics and a model of the Martian atmosphere.

The mass and speed distributions of particles that are ejected from a crater was calculated by using the data on crater ejecta presented in references 2 and 3. In these references the authors were concerned with the secondary particle environment on the moon. The moon has no atmosphere to alter the particles after they are ejected from the craters. Mars has a thin atmosphere which absorbs some of the kinetic energy of the ejecta particles before they return to the surface where secondary impacts can occur. The final mass and speed of the ejecta particles were determined by applying equations of meteor physics to the ejecta particles. The final mass and speed distributions define the secondary particle environment on Mars. A distinction is made between ejecta particles and secondary particles in this paper. Ejecta particles are particles that are ejected from a crater. Secondary particles are ejecta particles which impact on the surface. Not all ejecta particles become secondary particles, some escape the planet and some are completely ablated in the atmosphere. The particles that do impact the surface have less kinetic energy than when they were ejected from the crater. In order to compare the hazard that secondary particles present to a spacecraft with the hazard of meteoroids in space, the penetration fluxes for single-wall and double-wall aluminum structures were calculated for both environments.

METEOROID IMPACTS ON THE UPPER ATMOSPHERE OF MARS

Meteoroids are classified as either cometary or asteroidal depending on their origin. Meteoroids of cometary origin are assumed to have a representative density of 500 kg/m^3 whereas meteoroids of asteroidal origin are assumed to have a density of 3500 kg/m^3 (ref. 5). From reference 5, the flux of cometary meteoroids on the Martian atmosphere was calculated to be

$$\log_{10} \phi_c = -18.536 - 1.213 \log_{10} m \qquad (m > 10^{-9} \text{ kg}) \qquad (1)$$

$$\log_{10} \phi_c = -20.185 - 1.962 \log_{10} m - 0.063\left(\log_{10} m\right)^2 \qquad (10^{-15} \text{ kg} \leq m \leq 10^{-9} \text{ kg}) \qquad (2)$$

$$\log_{10} \phi_c = -4.930 \qquad (m < 10^{-15} \text{ kg}) \qquad (3)$$

where ϕ_c is the flux in number/m^2s of meteoroids of mass m and greater expressed in kilograms. The flux of asteroidal meteoroids was calculated to be

$$\log_{10} \phi_a = -17.10 - 0.84 \log_{10} m \qquad (m \geq 10^{-12} \text{ kg}) \qquad (4)$$

$$\log_{10} \phi_a = -7.02 \qquad (m < 10^{-12} \text{ kg}) \qquad (5)$$

where ϕ_a is the flux in number/m^2s.

The speed distribution for the meteoroids is not given in reference 5; therefore, the speed distributions given in table I were assumed for cometary and asteroidal meteoroids at Mars. The speed distribution for cometary meteoroids is based on the speed distribution of near-earth meteoroids given in reference 6, the range of speeds being adjusted so that the lower limit was equal to the escape velocity of Mars and the upper limit was equal to the collision velocity which Mars would have with a cometary particle in a retrograde parabolic orbit. The speed distribution for asteroidal meteoroids was determined from calculations of the impact speeds with which the large visible asteroids would strike Mars if their orbits were in the orbital plane of Mars and if their positions in orbit were altered so that an encounter would occur. It was assumed that the speed distribution and mass distribution of meteoroids are independent. It was also assumed that the angle at which the meteoroids enter the Martian atmosphere is random.

METEOROID IMPACTS ON THE SURFACE OF MARS

The meteoroids which strike the surface of Mars have lost some kinetic energy while passing through the Martian atmosphere. The effect that the Martian atmosphere has on meteoroids was calculated by using the following equations of meteor physics and the model of the Martian atmosphere shown in figure 1.

$$\frac{dm}{dt} = \frac{-4AC_1 m^{2/3} T^{-1/2}}{\delta^{2/3}} e^{-C_3/T} \qquad (6)$$

$$\frac{dV}{dt} = \frac{-\Gamma A \rho V^2}{\delta^{2/3} m^{1/3}} \qquad (7)$$

$$\frac{dT}{dt} = \frac{m^{2/3}}{m_1}\left(\frac{1}{2}\frac{A\Lambda\rho V^3}{C_2\delta^{2/3}} - \frac{4A\epsilon\sigma T^4}{C_2\delta^{2/3}} - \frac{4AC_1QT^{-1/2}}{C_2\delta^{2/3}}e^{-C_3/T}\right) \tag{8}$$

$$\frac{dH}{dt} = -V\cos\theta \tag{9}$$

These four basic equations of meteor physics describe the motion and ablation of a nonfragmenting meteoroid penetrating an atmosphere at some zenith angle θ. With the exception of equation (8), the equations as shown can be found in reference 7.

Equation (8) represents the energy balance of the system; the total energy received by the meteoroid from collisions with atmospheric molecules is expended on heating the body, on radiation from the body, and on evaporation of the body. This equation can be used to calculate the change in absolute temperature of the meteoroid surface with time which, in turn, is used in equation (6) to determine the ablation rate of the meteoroid.

Equation (8) as it appears in reference 7 is good for small meteoroids (<0.005 m in radius) which are assumed to heat uniformly. For meteoroids greater than 0.005 m in radius, equation (8) as it appears in this paper has an additional parameter m_1 which represents the mass of the meteoroid material outer shell heated to a uniform temperature. The thickness of the meteoroid outer shell is 0.005 m and remains constant as the meteoroid surface recedes because of ablation.

Some of the parameters appearing in equations (6) to (9) need more definition than that provided in the section "Symbols." The dimensionless meteoroid shape factor A is defined so that $A(m/\delta)^{2/3}$ is equal to the effective cross-sectional area of the meteoroid. For a spherical body, A is 1.21. The heat of ablation Q used in this paper is 1.36×10^6 J/kg. This value is the heat of ablation obtained by fusion and spraying of the meteoroid. If a higher heat of ablation had been chosen (that is, heat of ablation by vaporization on the spot), the ablation rate of the meteoroid would be lower. It is felt that taking this smaller value will help to compensate for fragmentation of the meteoroid. The drag coefficient Γ varies between 0.5 in continuum flow to 1.0 in free molecular flow. Between these limits the drag coefficient is given by a power law. (See "Symbols.") The heat-transfer coefficient Λ is a measure of the efficiency of the collision process in converting kinetic energy to heat (ref. 8), and is forced to lie between 0.1 in free continuum flow to 1.0 in free molecular flow.

The four meteor physics equations (eqs. (6) to (9)) were used in a numerical analysis to determine whether the residual kinetic energy of meteoroids striking the surface of Mars exceeded various levels. Calculations were begun at an initial altitude of 9×10^4 m, with an initial temperature of 280 K, an initial mass, an initial speed, and

an entry angle. The entry angle remained constant because the force of gravity was neglected as was the curvature of the planet surface. The changes in meteoroid mass, speed, temperature, and altitude were calculated for a small time interval, 10^{-4} s for cometary meteoroids and 10^{-3} s for asteroidal meteoroids, and the calculation repeated until the kinetic energy dropped below the level being tested or until the meteoroid struck the surface. The small time intervals were required because heating and deceleration rates were often very high; as a result, the analysis became unstable when greater time intervals were used. Many initial conditions of meteoroid mass, speed, and entry angle were tested and the initial conditions which resulted in various levels of residual kinetic energy are shown in figures 2 and 3. A meteoroid with initial mass and speed corresponding to a point above a particular curve will have a residual kinetic energy in excess of the value indicated for that curve. The curves in figure 2 are for cometary meteoroids; those in figure 2(a), with a normal entry angle and those in figure 2(b), with an entry angle 1.05 rad from the normal. Figure 3 is for asteroidal meteoroids; figure 3(a) presents the curves for those with a normal entry angle and figure 3(b), those with an entry angle 1.05 rad from the normal. When the entry angle is off the normal, greater initial masses are required to have the same residual kinetic energy. The only differences in the analyses for cometary and asteroidal meteoroids were the density of the meteoroid and the time interval used. A shorter time interval was required for cometary meteoroids in order to keep the analysis stable.

The flux of meteoroids on the Martian surface with kinetic energy in excess of a particular level was calculated by a numerical solution to the equation

$$\phi_E = \int_{\theta=0}^{\pi/2} d\theta \int_{V=0}^{\infty} dV \int_{m=f(V,\theta)}^{\infty} \frac{\partial \phi}{\partial m} g(V)\, h(\theta)\, dm$$

where $\partial\phi/\partial m$ is the differential mass-flux distribution function, $g(V)$ is the meteoroid speed probability density function, $h(\theta)$ is the meteoroid impact angle probability density function, and $m = f(V,\theta)$ is the equation for the initial conditions required to obtain the particular residual kinetic energy level being considered, that is, the equation for a curve like those in figures 2 and 3 except in three dimensions (mass, speed, and entry angle). The calculations were made for many kinetic-energy levels and generated the curves for meteoroid flux on the surface of Mars as a function of kinetic energy which are shown in figure 4. The two solid lines are the flux of cometary and asteroidal meteoroids on the surface of Mars. The two dashed lines are the flux of cometary and asteroidal meteoroids on the upper atmosphere of Mars. It can be seen that the Martian atmosphere is an effective shield against meteoroids. The total meteoroid flux on the surface of Mars is 10 orders of magnitude less than the flux on the upper atmosphere. The Martian atmosphere has a significant effect on cometary meteoroids with kinetic

energies less than 10^{15} J and asteroidal meteoroids with kinetic energies less than 10^{11} J. Notice that the flux of cometary meteoroids is greater than the flux of asteroidal meteoroids on the upper atmosphere for kinetic energies less than 10^{5} J, but notice that on the surface, the flux of asteroidal meteoroids is more than an order of magnitude greater than cometary meteoroids at any kinetic energy.

It can be seen in figure 4 that the total penetration flux through the Martian atmosphere, that is, the total flux on the Martian surface, is 1.34×10^{-15} penetrations/m^2s. Calculation of the penetration flux for aluminum plates by the method described in a subsequent section on the penetration hazard showed that a 0.067-m-thick aluminum shell surrounding Mars would have the same penetration flux. The Martian atmosphere has a mass per unit area equivalent to a 0.038-m-thick aluminum shell. Therefore, on a mass basis, the Martian atmosphere is 76 percent more efficient than an aluminum shell in reducing the meteoroid penetration flux.

PARTICLES EJECTED FROM CRATERS ON MARS

Data on the mass and speed distribution of particles ejected from hypervelocity impact craters in basalt were presented in reference 2. These data along with a few assumptions were the basis for the equations presented in reference 3 to describe the mass and speed of ejecta particles. The equations used in this paper are the same as those used in reference 3 and these equations are described in the following paragraph.

The total mass of material ejected from a crater M_e is

$$M_e = k_1\left(\frac{1}{2}V^2\right)m \tag{10}$$

where $k_1 = 10^{-4.9}$ s^2/m^2, V is the impact speed in m/s, and m is the mass of the meteoroid in kilograms. Note that the total mass ejected depends on the kinetic energy of the impacting meteoroid. It was because of this relationship that the flux of meteoroids on the surface was calculated in terms of kinetic energy in the preceding section. The largest particle ejected from a crater m_b is

$$m_b = 0.2M_e$$

The cumulative mass of ejecta particles that have mass m_e or smaller, due to a single impact m' is

$$m' = M_e\left(\frac{m_e}{m_b}\right)^{0.2}$$

The cumulative mass of ejecta particles that have speed V_e or greater, due to a single impact $\overline{m}$ is

$$\overline{m} = M_e\, G(V_e)$$

The function $G(V_e)$ is plotted in figure 5. One of the assumptions made in reference 3 is that the ejecta are distributed so that the smaller the ejecta particle, the faster it travels. From this assumption it follows that

$$m' = \overline{m}$$

The angle at which the ejecta are thrown out of a crater was measured in reference 2 and was found to be a single-valued function of the ejecta speed. (See fig. 6.)

The value of the maximum speed of the ejecta and hence the value of the corresponding minimum mass ejected is not defined by the curve in figure 5. For the purposes of this paper, the maximum speed of the ejecta particles was assumed to be 20 000 m/s. This arbitrary choice of the maximum ejecta speed does not affect the results obtained in this paper because the calculations in the following section showed that all ejecta particles with speeds greater than 20 000 m/s were ablated to masses less than 10^{-9} kg, the lower limit of particle masses considered in this paper. As a point of interest, these calculations show that very small ejecta particles would not significantly affect the penetration hazard even in the absence of an atmosphere because the kinetic energy and momentum of ejecta particles decreases as the mass decreases even though the speed increases.

All the ejecta particles with speed in the small interval V_{e1} to V_{e2}, characterized by the speed $\frac{V_{e1} + V_{e2}}{2}$, which are ejected from a single crater formed by a meteoroid of kinetic energy E, have masses which can be characterized by the mass

$$m_e = 0.2k_1 E\left[G\left(\frac{V_{e1} + V_{e2}}{2}\right)\right]^5$$

The flux of ejecta particles with speed $\frac{V_{e1} + V_{e2}}{2}$ and the corresponding mass m_e which are ejected from all craters formed by meteoroids whose kinetic energy can be characterized as E is

$$\phi_{\frac{V_{e1}+V_{e2}}{2},m_e} = \phi_E N_{V_{e1}-V_{e2}}$$

where $N_{V_{e1}-V_{e2}}$ is the number of ejecta particles with speed in the range V_{e1} to V_{e2} which are ejected from a single crater, and ϕ_E is the flux on the surface of meteoroids of energy E or greater. The value of $N_{V_{e1}-V_{e2}}$ is

$$N_{V_{e1}-V_{e2}} = \frac{M_e G(V_{e1}) - M_e G(V_{e2})}{m_e}$$

so that

$$\phi_{\frac{V_{e1}+V_{e2}}{2},m_e} = \phi_E \frac{5\left[G(V_{e1}) - G(V_{e2})\right]}{\left[G\left(\frac{V_{e1}+V_{e2}}{2}\right)\right]^5} \tag{11}$$

Equation (11) was used to calculate the flux of ejecta particles in small speed intervals from meteoroids having kinetic energies ranging from the minimum energy meteoroid which strikes the Martian surface $(10^4\ J)$ to the maximum energy meteoroid that would have struck Mars since the formation of the solar system 1.45×10^{17} s (4.6 billion years) ago. The maximum energy meteoroid was estimated from figure 4 by using the known area-time product of the Martian surface to be approximately 10^{25} J. This value gives an average ejecta flux over 1.45×10^{17} s which is greater than the average flux over a smaller time period because the contribution of rare high-energy meteoroids is included.

The flux of ejecta particles on Mars is presented in figure 7 in the form of the cumulative flux of particles of a given mass and greater. The mass distribution and speed distribution of the ejecta particles were not independent. The speed distributions of the ejecta particles for several mass ranges are presented in table II.

The equations describing ejecta particles are based on hypervelocity impact data using basalt targets. Therefore, it has been necessary to assume that the material on the surface of Mars behaves like basalt. Actually, much of Mars must be covered with a dust layer which is porous. It has been suggested in reference 3 that other hypervelocity impact data on porous surfaces, which unfortunately were not adequate to make a complete analysis, showed that the assumption that the surface behaves like basalt would cause the hazard of penetration from ejecta to be overestimated and therefore to be conservative.

Thus, in two respects, the consideration of rare high-energy meteoroids and the assumption that the surface of Mars behaves like solid basalt, this analysis is conservative.

SECONDARY PARTICLE IMPACT ON SURFACE OF MARS

The ejecta particles thrown out of meteoroid impact craters on Mars must pass through the Martian atmosphere before they can strike a spacecraft on the surface or strike the surface of Mars. The ejecta particles may be completely ablated in the atmosphere, may pass through the atmosphere and escape the planet, or may fall back and impact the surface. The particles, which fall back to the surface and present a potential hazard to spacecraft operating on the surface, will lose some kinetic energy while passing through the atmosphere.

The residual mass and speed of the ejecta particles, which are the mass and speed of the secondary particles, were determined by applying the equations of meteor physics (eqs. (6) to (9)) to the ejecta particles. The meteor physics equations were altered for this application to include the effect of gravity and the curvature of the planet surface. In this application the "meteor" particle starts at the surface with an initial speed and an initial angle depending on that speed (see fig. 6) and travels upward until it is completely ablated, escapes, or returns to the surface as a secondary particle.

The mass-flux of secondary particles is presented in figure 8. The flux can be approximated by the empirical equation

$$\log_{10} \phi_s = -13.999 - 0.790 \log_{10} m - 0.00502\left(\log_{10} m\right)^2 \tag{12}$$

where ϕ_s is the flux of secondary particles in number/m^2s with mass m or greater in kilograms. This equation is in agreement with the calculated values of the flux within an accuracy of 39 percent, the agreement being more accurate for most masses. The mass-flux of meteoroids on the upper atmosphere of Mars is also shown in figure 8 for comparison. The flux of meteoroids is predominantly of asteroidal origin for masses greater than 10^{-4} kg. The flux of secondary particles on the surface of Mars is greater than the flux of meteoroids on the Martian atmosphere by approximately three orders of magnitude for masses greater than 10^{-3} kg. The flux of secondary particles with masses greater than 10^{-9} kg (fig. 8), is essentially the same as the flux of ejecta particles (fig. 7).

The speed distribution of the secondary particles is presented in table III for several mass ranges because the mass distribution and speed distribution are dependent. The secondary particle speed probability density function can be approximated by the gamma density function

$$g(V) = \frac{a^3}{2} V^2 e^{-aV} \tag{13}$$

where $a = 0.0175 - 0.0059 \log_{10} m + 0.00074(\log_{10} m)^2$, V is the secondary particle speed in m/s, and m is the particle mass in kilograms. The agreement between the calculated probability density functions for speed, like those in table III, and the equation used to approximate them (eq. (13)) is shown in figure 9. The constants in the equation were chosen so that the penetration flux calculated in the next section by using the equation would agree with calculations in which the calculated speed distributions, that is, the histograms in figure 9, were used. The agreement is within 79 percent for thicknesses between 2×10^{-4} m and 10^{-2} m, whereas the penetration flux is overestimated for thinner material when the equation is used, being a factor of 3 too great at a thickness of 10^{-5} m. The speed of the secondary particles is significantly less than the speed of the ejecta particles and thus shows that the effect of the Martian atmosphere on ejecta particles larger than 10^{-9} kg was primarily a reduction in speed and little reduction in mass. The speed of the secondary particles is much lower than the speed of meteoroids.

The analysis showed that very few particles are able to escape the planet. Only ejecta particles with masses greater than 1 kg and with speed in the 6000 to 7000 m/s range at an angle of 0.73 to 0.77 rad from the normal were able to escape. These particles escape with more than 75 percent of their initial mass.

SECONDARY PARTICLE PENETRATION HAZARD ON MARS

The penetration hazards to aluminum structures, single wall and double wall, from secondary particles were calculated and compared with the penetration hazard from meteoroids to structures outside of the Martian atmosphere. For a spacecraft resting on the Martian surface, the penetration hazard from meteoroids is negligible compared with the penetration hazard from secondary particles. See the section "Comparison of Penetration Hazard on the Martian Surface and Lunar Surface."

The penetration flux for aluminum was calculated by using the equation,

$$\psi_p = \int_{\theta=0}^{\pi/2} d\phi \int_{V=0}^{\infty} dV \int_{m=p(\theta,V)}^{\infty} \frac{\partial \phi}{\partial m} g(V)\, h(\theta)\, dm \qquad (14)$$

where $\partial\phi/\partial m$ is the differential mass-flux distribution function, $g(V)$ is the meteoroid speed probability density function, $h(\theta)$ is the meteoroid impact angle probability density function, and $m = p(\theta,V)$ is the penetration equation for the structure. Equation (14) is developed in reference 9.

The empirical penetration equation used for single aluminum walls when the normal component of the impact velocity was greater than 167 m/s is

$$m = \frac{4.33 \times 10^{10} \ell^{2.84}}{(V \cos \theta)^{2.485}}$$

where m is the minimum mass meteoroid in kilograms which will penetrate an aluminum plate of thickness ℓ in meters, when the impact speed is V in meters per second, and the impact angle is θ, measured from the normal. This equation is the Fish and Summers penetration equation from reference 6 altered to include the effect of impact angle.

The Fish and Summers equation is based on hypervelocity impact tests. It was not intended to be used for the low-speed impacts which are typical for most of the secondary particles. The penetration equation used for single- and double-wall aluminum structures when the normal component of the impact velocity was less than 167 m/s is

$$m = \frac{1.29 \times 10^{22} \ell^{2.84}}{(V \cos \theta)^{7.66}}$$

where again m is in kilograms, ℓ is in meters, and V is in meters per second. This equation was based on impact tests in which single- and double-wall aluminum targets were struck with spherical aluminum projectiles at speeds from 90 to 1600 m/s at normal impact angles. The data from the tests are shown in figure 10. The data points show joint conditions of mass and speed which will create a threshold penetration. The Fish and Summers equation is in good agreement with the data at impact speeds greater than 167 m/s. However, the data at speeds less than 167 m/s showed that a different equation was needed in the low speed range. Notice that at all speeds less than 1600 m/s, single- and double-wall structures have the same penetration resistance. At these low speeds the projectiles are not fragmented by the bumper so that no bumper effect occurs and penetration depends only on the total thickness of the structure, which was the same for all the structures shown in figure 10.

The penetration flux for single-wall aluminum structures outside the Martian atmosphere is the sum of the cometary penetration flux and asteroidal penetration flux and was calculated by using the mass distribution of these meteoroids given by equations (1) to (5) and the speed distributions given in table I. The penetration fluxes for single- and double-wall structures from secondary particles were calculated by using the mass distribution given by equation (12) and the speed distribution by equation (13). In all cases the impact angles were assumed to be random.

The results of these calculations are presented in figure 11 where the ratio of the penetration flux from secondary particles for a spacecraft on the surface to the penetration flux from meteoroids for a spacecraft outside the atmosphere is shown as a function

of the thickness of the structure. The penetration flux from secondary particles is essentially the total penetration flux for a structure on the surface of Mars because the penetration flux from meteoroids is negligible on the surface of Mars. For double-wall structures, the thickness is the actual thickness of the two aluminum sheets. The efficiency factor of a double-wall structure is the ratio of the single-wall thickness which has the same penetration flux as the double wall to the actual thickness of the double wall. A double-wall structure may have a high efficiency factor in an environment of high-speed meteoroids because the outer wall or bumper shatters the meteoroid and the fragments are dispersed over a large area of the second wall; this dispersion causes a large number of small craters instead of a single deep crater which could completely penetrate the second wall. The data in figure 10 show that when the impact speed is too low to shatter the particle, a double wall behaves like a single wall of the same thickness, that is, the efficiency factor is 1. Therefore, a double-wall structure which has a high efficiency factor against meteoroids will have an efficiency factor of 1 against secondary particles. It can be seen in figure 11 that the penetration flux for a single aluminum wall in the 10^{-5} to 10^{-2} m thickness range is much less for a spacecraft on the surface of Mars than it would be for a spacecraft in space near Mars. However, a double-wall structure with an efficiency factor of 10 would have a greater penetration flux on the surface of Mars than in space near Mars if the wall thickness exceeded 7×10^{-4} m.

COMPARISON OF PENETRATION HAZARD ON THE MARTIAN SURFACE AND LUNAR SURFACE

The penetration flux for single aluminum plates, 10^{-5} to 10^{-2} m thick, was calculated in the space near the Moon and on the lunar surface. The interplanetary meteoroid environment model (ref. 5) was used to determine the flux of meteoroids on the lunar atmosphere. (See fig. 12.) The meteoroid flux on the lunar surface was assumed to be equal to the flux on the atmosphere because the lunar atmosphere is extremely thin and should have a negligible effect on the meteoroids. The flux of secondary particles on the Moon was calculated in the same manner as the flux of secondary particles on Mars except that no ablation or deceleration of ejecta particle was considered on the Moon. The penetration flux for aluminum plates from meteoroids and secondary particles is presented in figure 13 for Mars and the Moon.

The penetration flux for 10^{-5}- to 10^{-2}-m-thick aluminum plates in space near the Moon is slightly greater than the penetration flux in space near Mars (fig. 13) because the flux of meteoroids with kinetic energies necessary to penetrate these plates, 10^{-7} to 10^{4} J, is slightly greater near the Moon than near Mars (fig. 12).

The penetration flux from meteoroids is much greater on the lunar surface than on the Martian surface (fig. 13) because the flux of meteoroids with kinetic energies in the 10^{-7} to 10^{4} J range is greatly reduced by the Martian atmosphere (fig. 12).

The penetration flux from secondary particles is greater on the lunar surface than on the Martian surface except for thicknesses near 10^{-2} m. (See fig. 13.) For thicknesses greater than 10^{-2} m, the penetration flux from secondary particles is greater on Mars than on the Moon. Most of the secondary particles which can penetrate 10^{-5}- to 10^{-2}-m-thick aluminum plates are produced by meteoroids which impact with kinetic energies greater than 10^{7} J. The flux of meteoroids with kinetic energies in excess of 10^{7} J is slightly greater on Mars than on the Moon (fig. 12), however, the Martian atmosphere greatly decelerates the small secondary particles produced and causes the penetration flux from secondary particles to be greater on the Moon for thin plates. The secondary particles capable of penetrating a 10^{-2}-m aluminum plate are large and affected only slightly by the Martian atmosphere; therefore, the penetration flux for thick plates is greater on Mars than on the Moon.

The total penetration flux for aluminum plates on the surface of the Moon and Mars is shown in figure 14. The total penetration flux is the sum of the meteoroid and secondary particle penetration fluxes. In the case of Mars, the meteoroid flux on the surface is negligible compared with the secondary particle flux, whereas on the Moon, just the opposite is true. The penetration hazard on the surface of the Moon is essentially the same as that in space near the Moon, whereas the penetration hazard on the surface of Mars is much less than the hazard in space near Mars. The total penetration flux on the surface of Mars is much lower than that on the surface of the Moon.

CONCLUDING REMARKS

The Martian atmosphere is an effective shield against meteoroids, and reduces the total flux on the surface by 10 orders of magnitude. The Martian atmosphere also appreciably decelerates the particles ejected from meteoroid craters.

The flux of secondary particles on Mars can be approximated by the equation

$$\log_{10} \phi_s = -13.999 - 0.790 \log_{10} m - 0.00502 \left(\log_{10} m\right)^2$$

where ϕ_s is the flux of particles in number/m^2s with mass m or greater in grams and the speed distribution can be approximated by the equation

$$g(V) = \frac{a^3}{2} V^2 e^{-aV}$$

where

$$a = 0.0175 - 0.0059 \log_{10} m + 0.00074(\log_{10} m)^2$$

$g(V)$ is the particle speed probability density function, V is the speed in m/s, and m is the mass in kilograms. The assumptions made in developing this model of the secondary particle environment on Mars were conservative; that is, they tended to cause the hazard to be overestimated. However, there are uncertainties in the meteoroid environment model and it is therefore not certain that this model is an upper limit for the secondary particle environment.

For a spacecraft on the surface of Mars, the penetration hazard from meteoroids is negligible compared with the penetration hazard from secondary particles. The penetration flux for single-wall aluminum structures, 10^{-5} to 10^{-2} m thick, on the surface of Mars due to secondary particles is small compared with the penetration flux the structure was subjected to while it was outside the Martian atmosphere. However, the penetration flux for double-wall structures on the surface may be greater, because of secondary particles, than the structure was subjected to while outside the Martian atmosphere, because the secondary particle speeds are low and bumpers are ineffective at low speeds.

The penetration hazard from meteoroids and secondary particles is much lower on the surface of Mars than it is on the surface of the Moon.

Langley Research Center,
National Aeronautics and Space Administration,
Hampton, Va., August 9, 1972.

REFERENCES

1. Dohnanyi, J. S.: Collisional Model of Meteoroids. TR-67-340-3 (Contract NASw-417), Bellcomm, Inc., July 1967. (Available as NASA CR-88864.)

2. Gault, Donald E.; Shoemaker, Eugene M.; and Moore, Henry J.: Spray Ejected From the Lunar Surface by Meteoroid Impact. NASA TN D-1767, 1963.

3. Zook, Herbert A.: The Problem of Secondary Ejecta Near the Lunar Surface. EN-8, Transactions of 1967 National Symposium on "Saturn V/Apollo and Beyond," Vol. I, Steve S. Hu, ed., Amer. Astronaut. Soc., c.1967.

4. Shoemaker, E. M.; Hait, M. H.; Swann, G. A.; Schleicher, D. L.; Dahlem, D. H.; Schaber, G. G.; and Sutton, R. L.: Lunar Regolith at Tranquility Base. Science, vol. 167, no. 3918, Jan. 30, 1970, pp. 452-455.

5. Anon.: Meteoroid Environment Model – 1970 [Interplanetary and Planetary]. NASA Vehicle Design Criteria (Environment). NASA SP-8038, 1970.

6. Anon.: Meteoroid Environment Model – 1969 [Near Earth to Lunar Surface]. NASA Space Vehicle Design Criteria (Environment). NASA SP-8013, 1969.

7. Lebedinec, V. N.; and Šuškova, V. B.: Evaporation and Deceleration of Small Meteoroids. Physics and Dynamics of Meteors, Ľubor Kresák and Peter M. Millman, eds., Springer-Verlag, 1968, pp. 193-204.

8. McCrosky, R. E.; and Soberman, R. K.: Results From an Artificial Iron Meteoroid at 10 km/s. Smithsonian Contrib. Astrophysics, vol. 7, 1963, pp. 199-208.

9. Humes, Donald H.: Calculation of the Penetration Flux for a Multiwall Structure on the Lunar Orbiter Spacecraft. NASA TN D-5455, 1969.

TABLE I.- SPEED DISTRIBUTION OF METEOROIDS

STRIKING MARTIAN ATMOSPHERE

Cometary speed range, m/s	Fraction	Asteroidal speed range, m/s	Fraction
5000 to 7420	0.046	5 000 to 10 000	0.50
7420 to 9830	.254	10 000 to 15 000	.30
9830 to 12 250	.257	15 000 to 20 000	.15
12 250 to 14 670	.140	20 000 to 25 000	.05
14 670 to 17 080	.093		
17 080 to 19 500	.056		
19 500 to 21 920	.048		
21 920 to 24 330	.030		
24 330 to 26 750	.018		
26 750 to 29 170	.012		
29 170 to 31 580	.010		
31 580 to 34 000	.006		
34 000 to 36 420	.004		
36 420 to 38 830	.003		
38 830 to 41 250	.002		
41 250 to 43 670	.003		
43 670 to 46 080	.004		
46 080 to 48 500	.004		
48 500 to 50 920	.004		
50 920 to 53 330	.002		
53 330 to 55 750	.003		
55 750 to 58 170	.001		

TABLE II.- SPEED DISTRIBUTION OF EJECTA PARTICLES ON MARTIAN SURFACE

Speed range, m/s	Fraction for a mass range of –			
	10^{-9} to 10^{-8} kg	10^{-6} to 10^{-5} kg	10^{-3} to 10^{-2} kg	10^{0} to 10^{1} kg
0 to 200	0.000	0.005	0.060	0.250
200 to 500	.061	.234	.430	.437
500 to 1000	.049	.084	.070	.055
1000 to 2000	.100	.120	.094	.072
2000 to 5000	.284	.213	.164	.126
5000 to 10 000	.250	.170	.131	.060
10 000 to 20 000	.256	.174	.051	.000

TABLE III.- SPEED DISTRIBUTION OF SECONDARY PARTICLES ON MARTIAN SURFACE

Speed range, m/s	Fraction for a mass range of –					
	10^{-9} to 10^{-8} kg	10^{-6} to 10^{-5} kg	10^{-3} to 10^{-2} kg	10^{0} to 10^{1} kg	10^{3} to 10^{4} kg	10^{6} to 10^{7} kg
0 to 10						
10 to 20	1.000					
20 to 30						
30 to 40		0.001		0.003	0.024	0.071
40 to 50		.704		.005	.028	.063
50 to 60		.270	0.001	.004	.019	.038
60 to 70		.025	.001	.010	.017	.028
70 to 80			.002	.009	.053	.079
80 to 90			.003	.010	.029	.036
90 to 100			.005	.016	.043	.051
100 to 200			.892	.226	.276	.266
200 to 300			.096	.276	.138	.128
300 to 400				.167	.130	.120
400 to 500				.019	.089	.083
500 to 600				.011	.022	.017
600 to 700				.010	.004	.005
700 to 800				.009	.005	.004
800 to 900				.015	.005	.003
900 to 1000				.016	.007	.005
1000 to 2000				.088	.058	.003
2000 to 3000				.073	.041	
3000 to 4000				.033	.012	

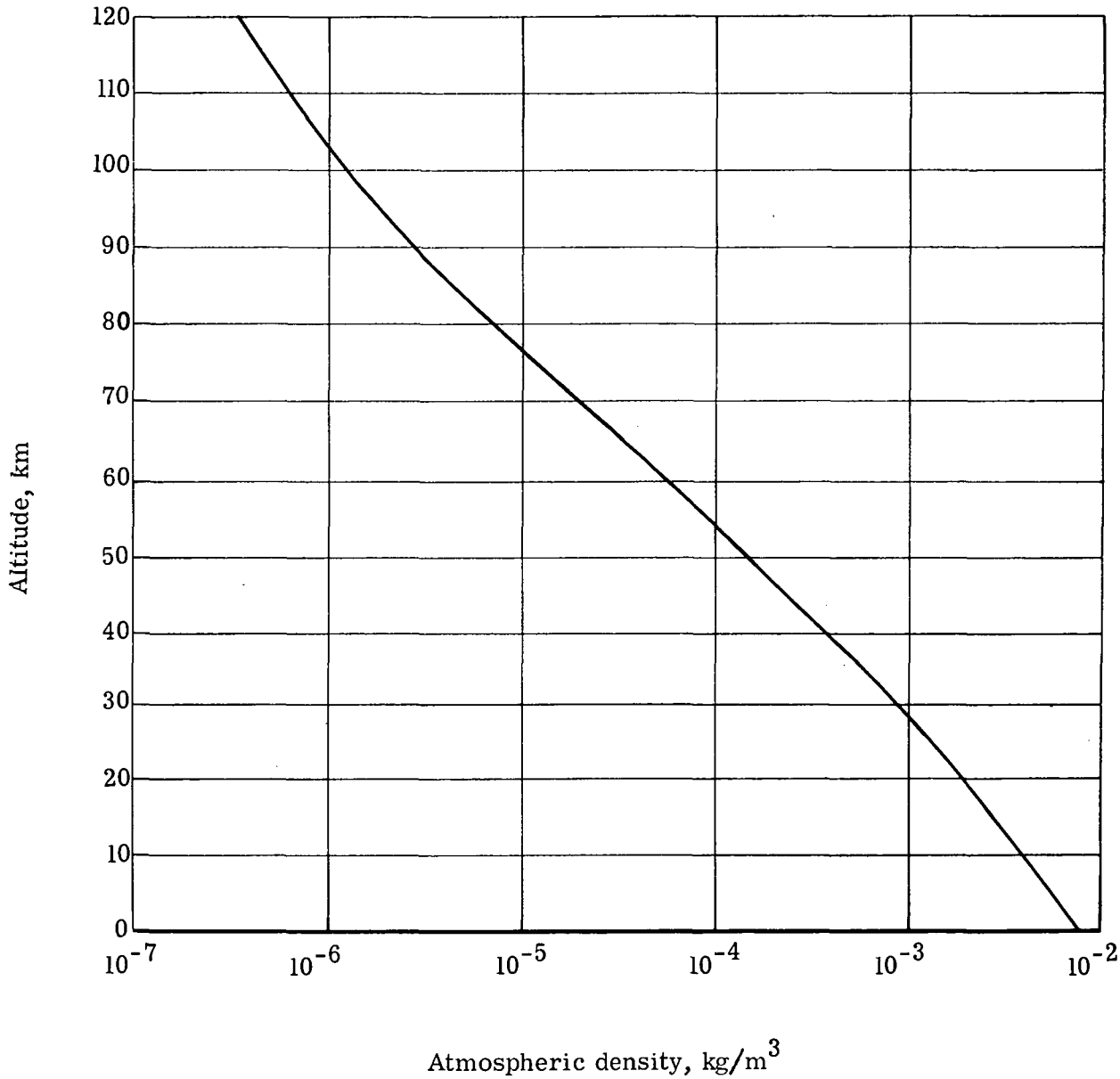

Figure 1.- Model of the Martian atmosphere.

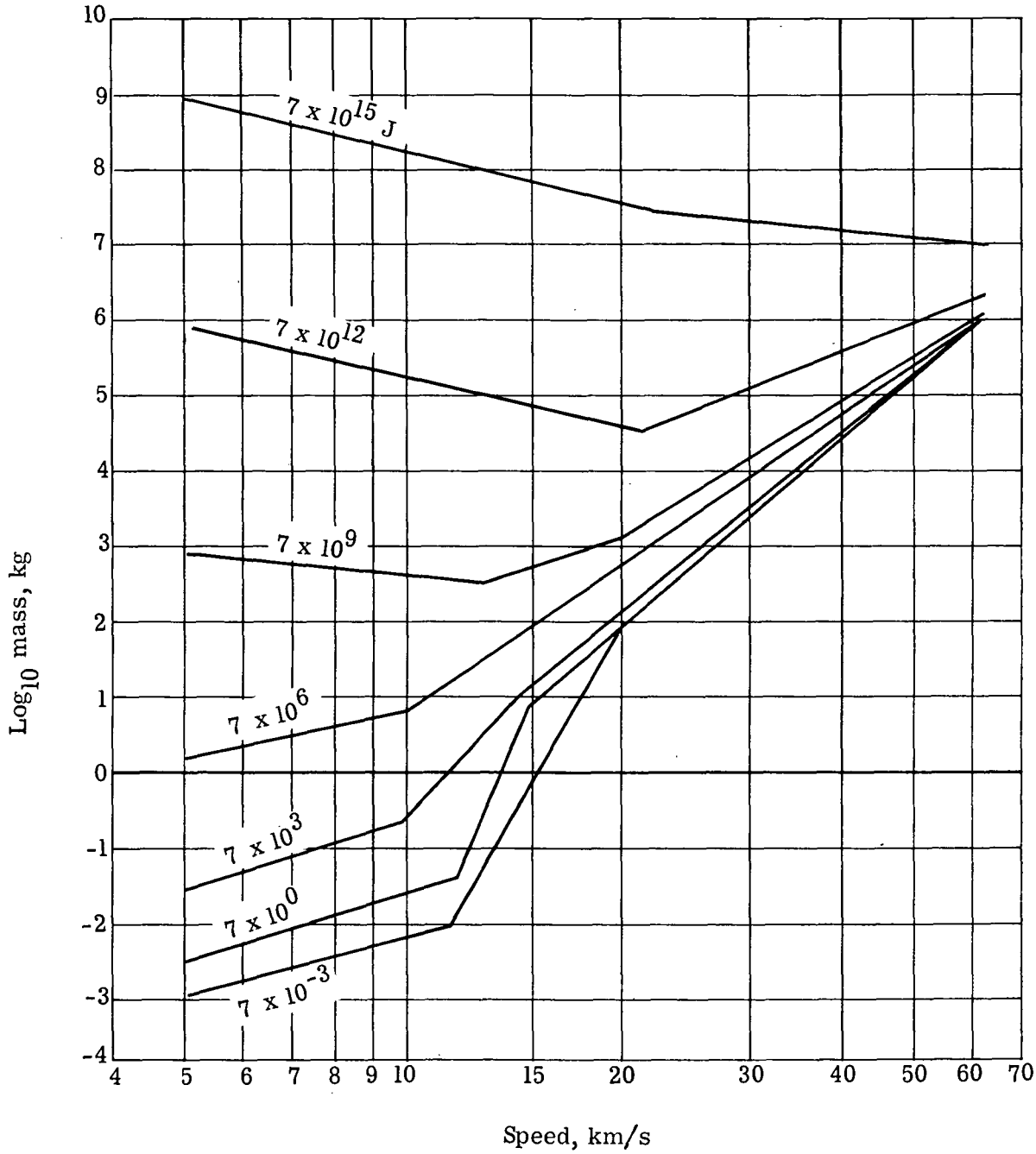

(a) Normal entry angle.

Figure 2.- Residual kinetic energy of cometary meteoroids after penetrating Martian atmosphere.

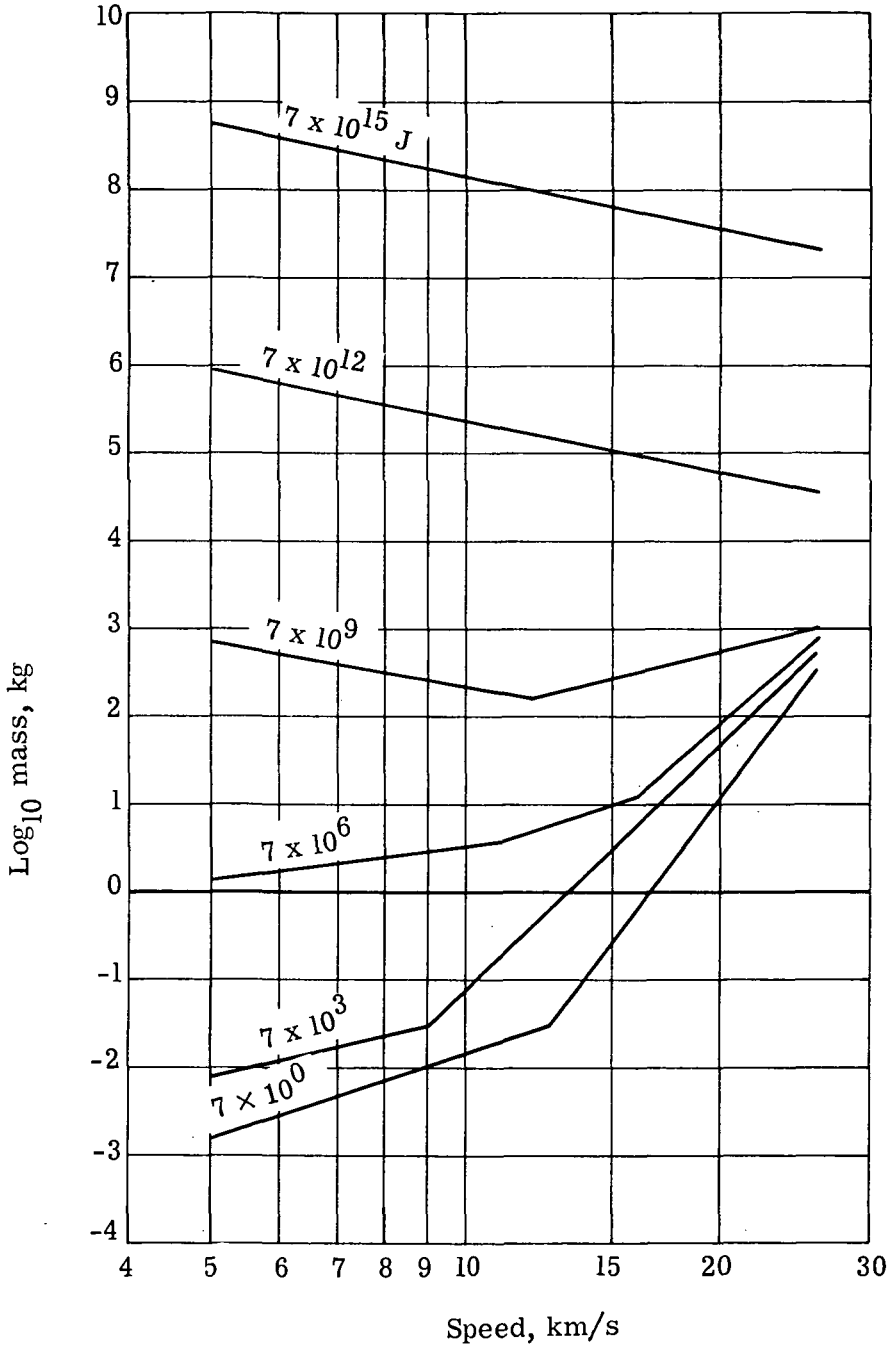

(b) Entry angle 1.05 rad from normal.

Figure 3.- Concluded.

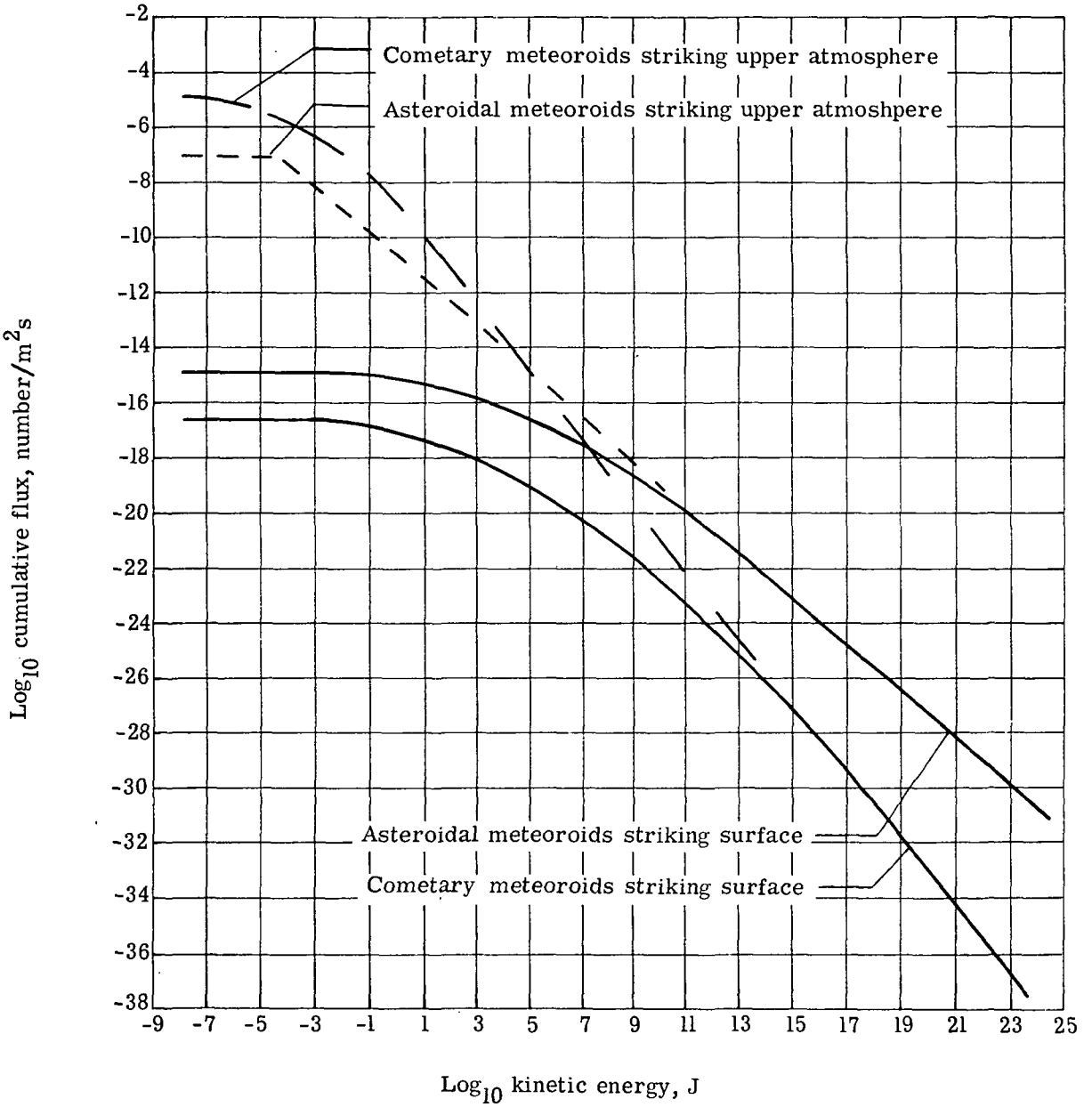

Figure 4.- Meteoroid flux on upper atmosphere and on surface of Mars.

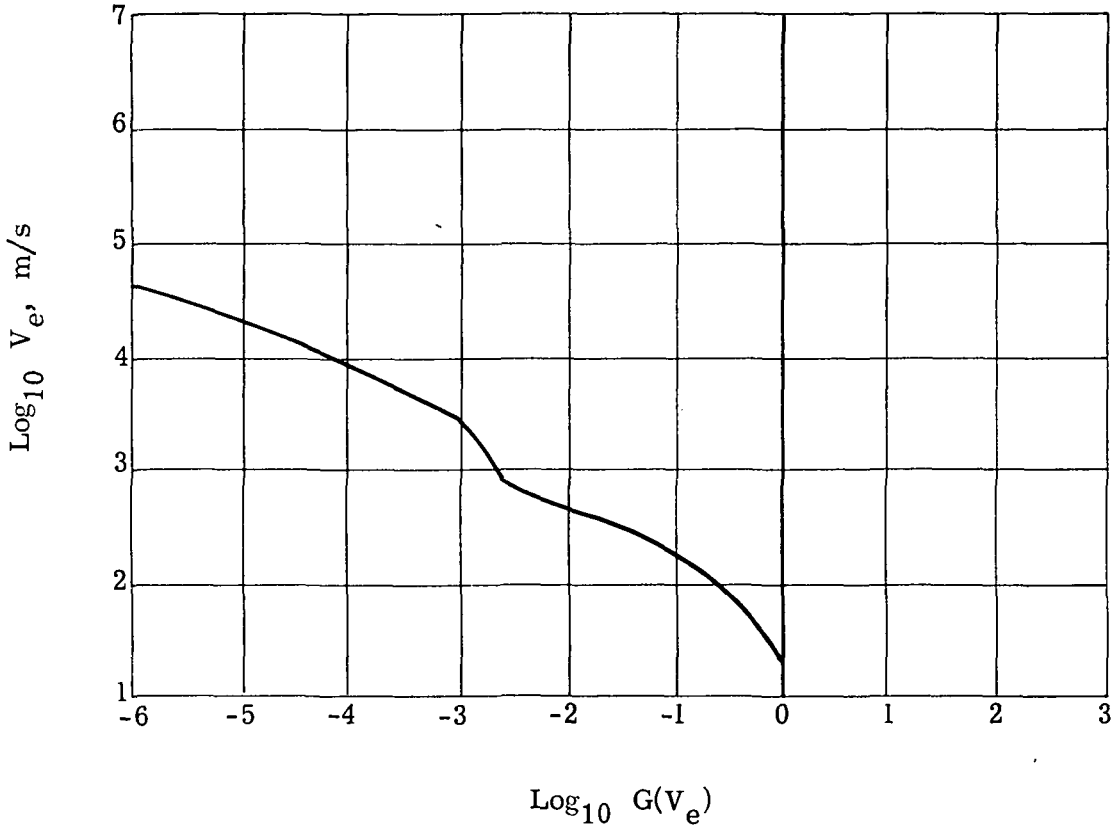

Figure 5.- Fraction of mass ejected in excess of a given speed for fragments thrown out of craters formed in basalt by hypervelocity impact. (From ref. 3.)

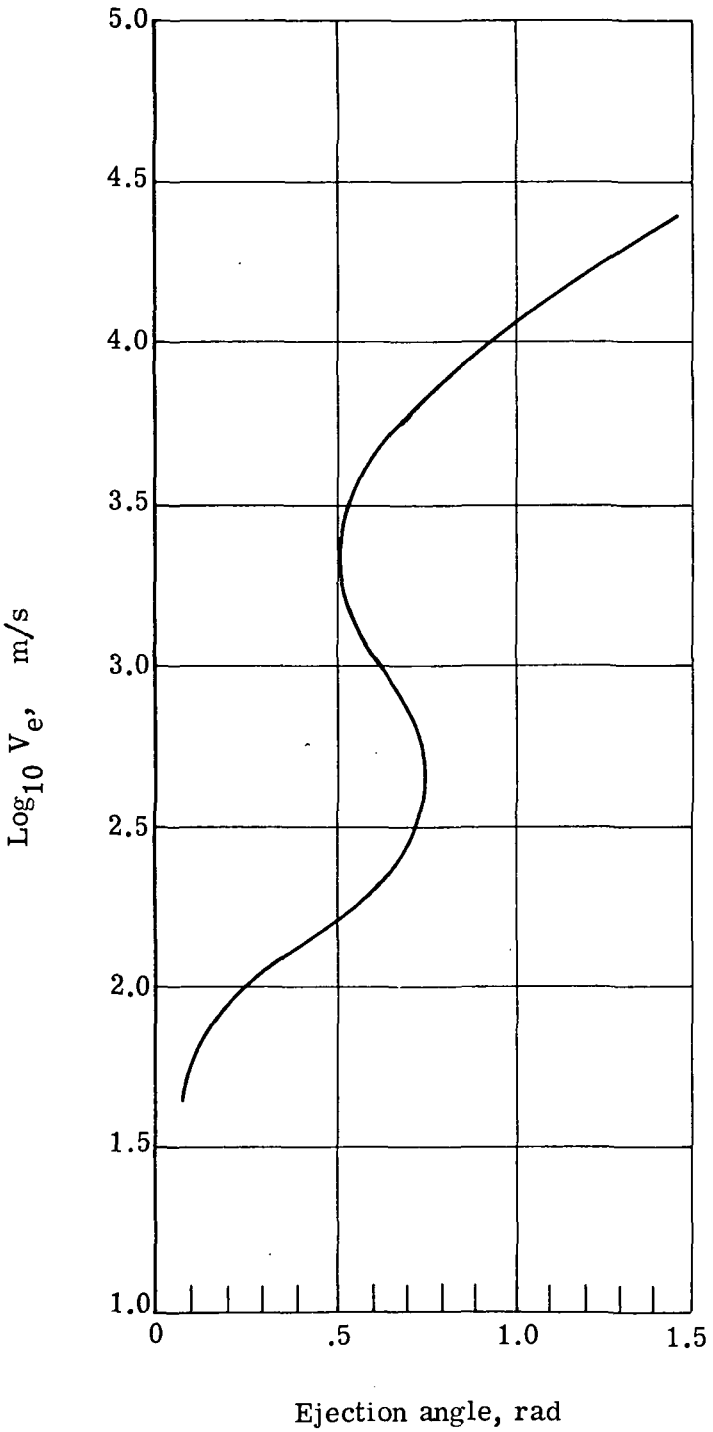

Figure 6.- Variation of ejection speed with ejection angle for fragments thrown out of craters formed in basalt by hypervelocity impact. (From ref. 2.) Angle is measured from the normal to the surface.

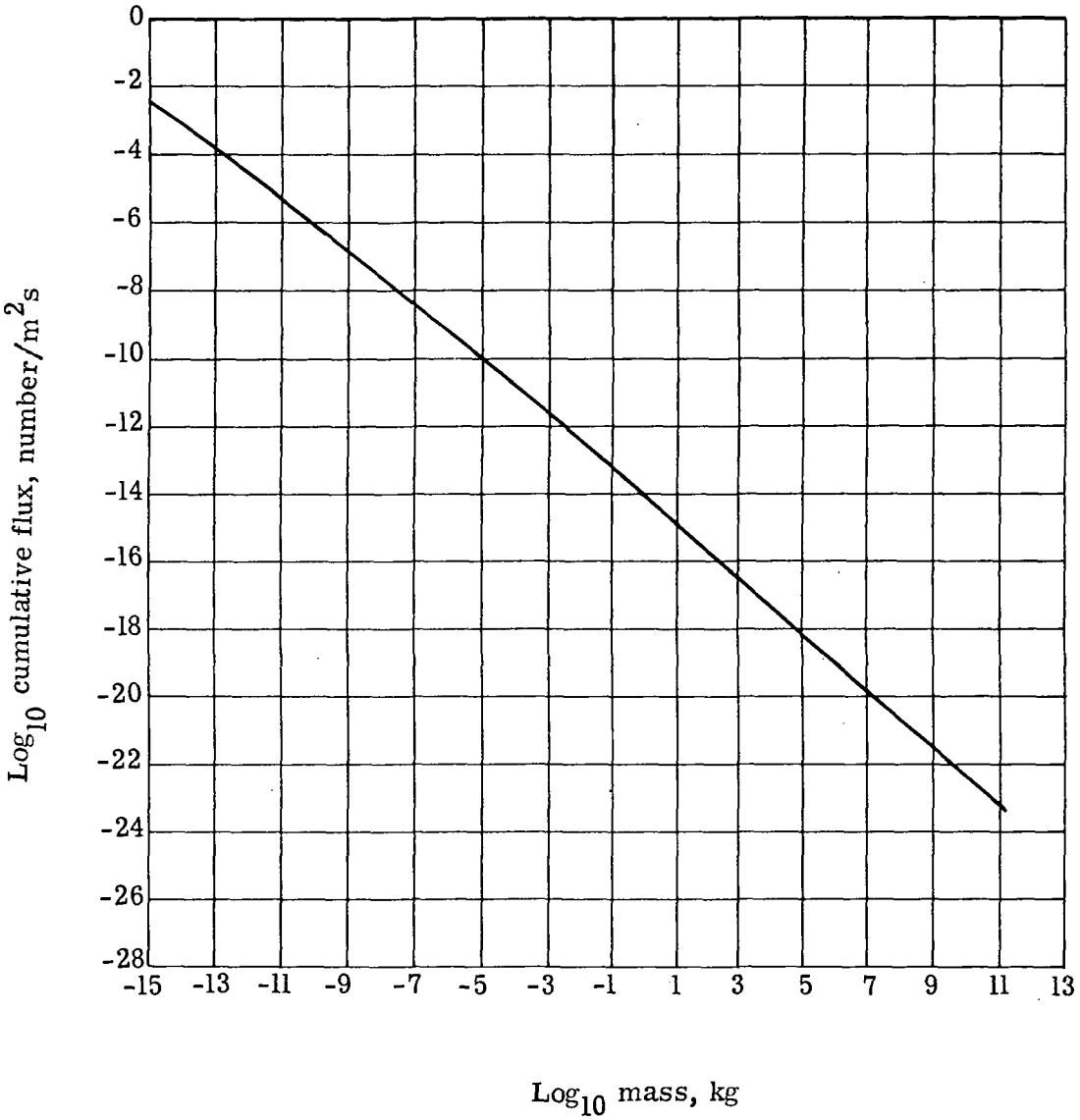

Figure 7.- Flux of ejecta particles from meteoroid craters on the Martian surface.

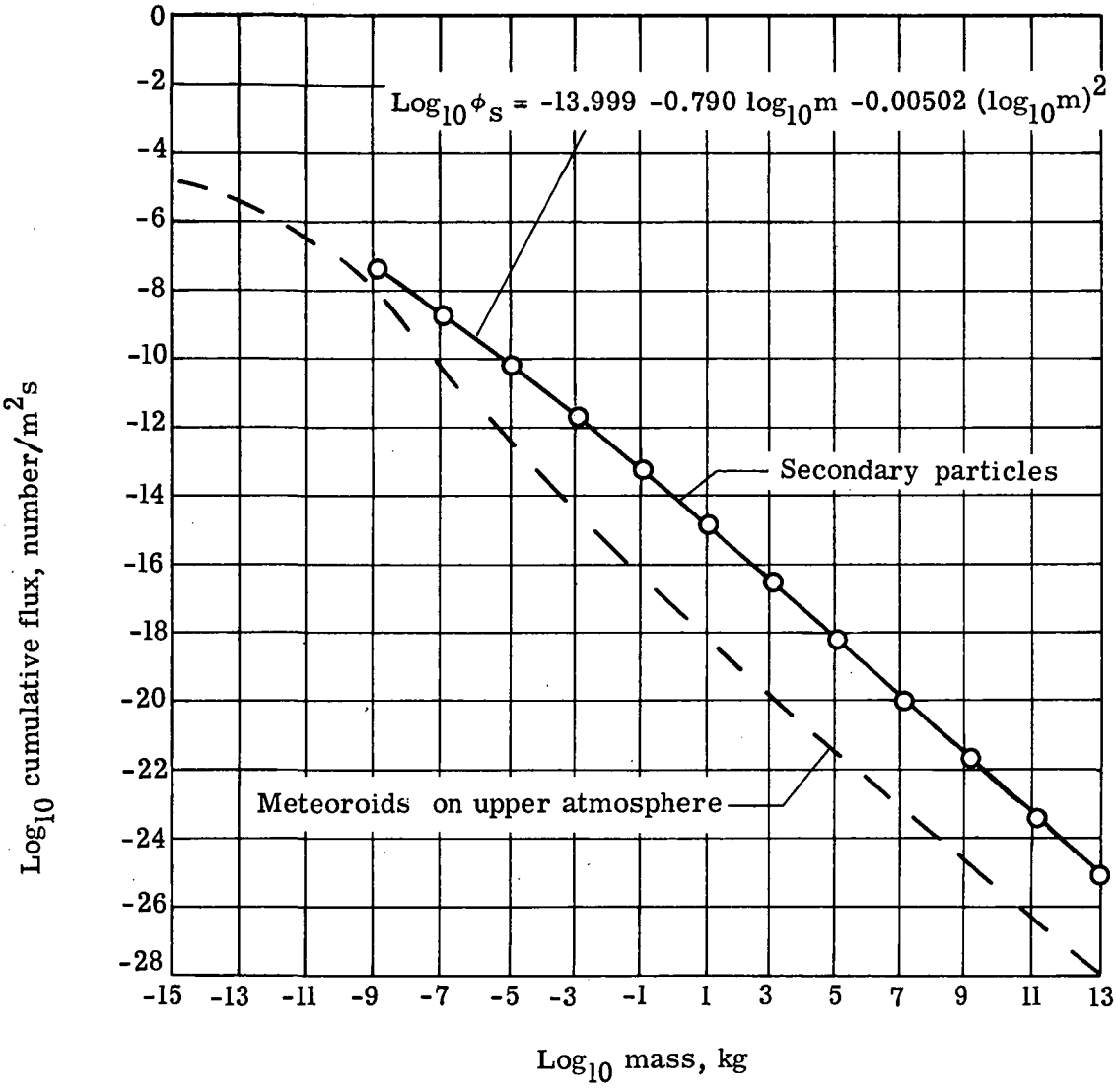

Figure 8.- Flux of secondary particles on Martian surface.

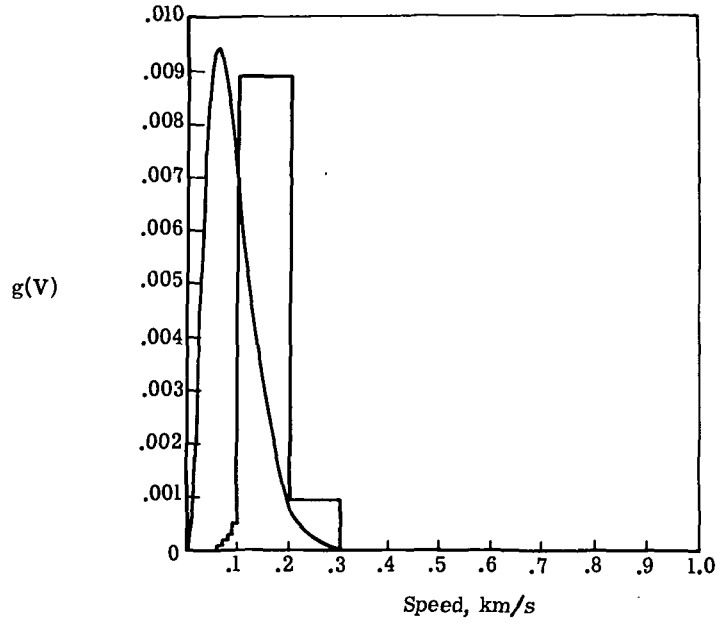

(a) 10^{-3} to 10^{-2} kg.

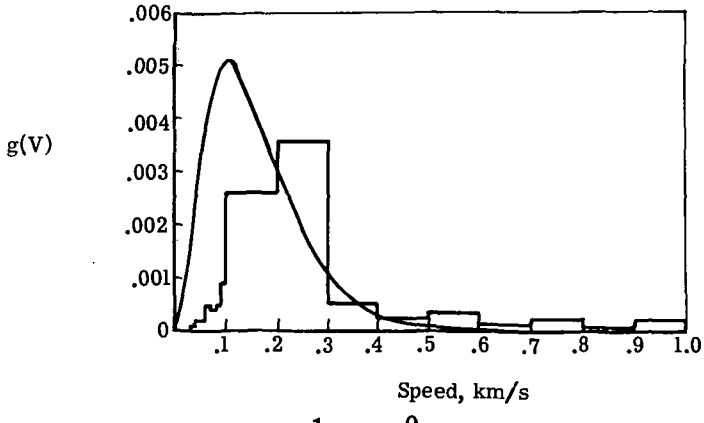

(b) 10^{-1} to 10^{0} kg.

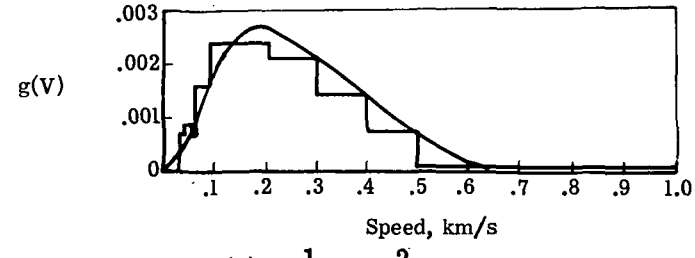

(c) 10^{1} to 10^{2} kg.

Figure 9.- Speed distribution of secondary particles, a comparison of the calculated results and the equation used to approximate the results.

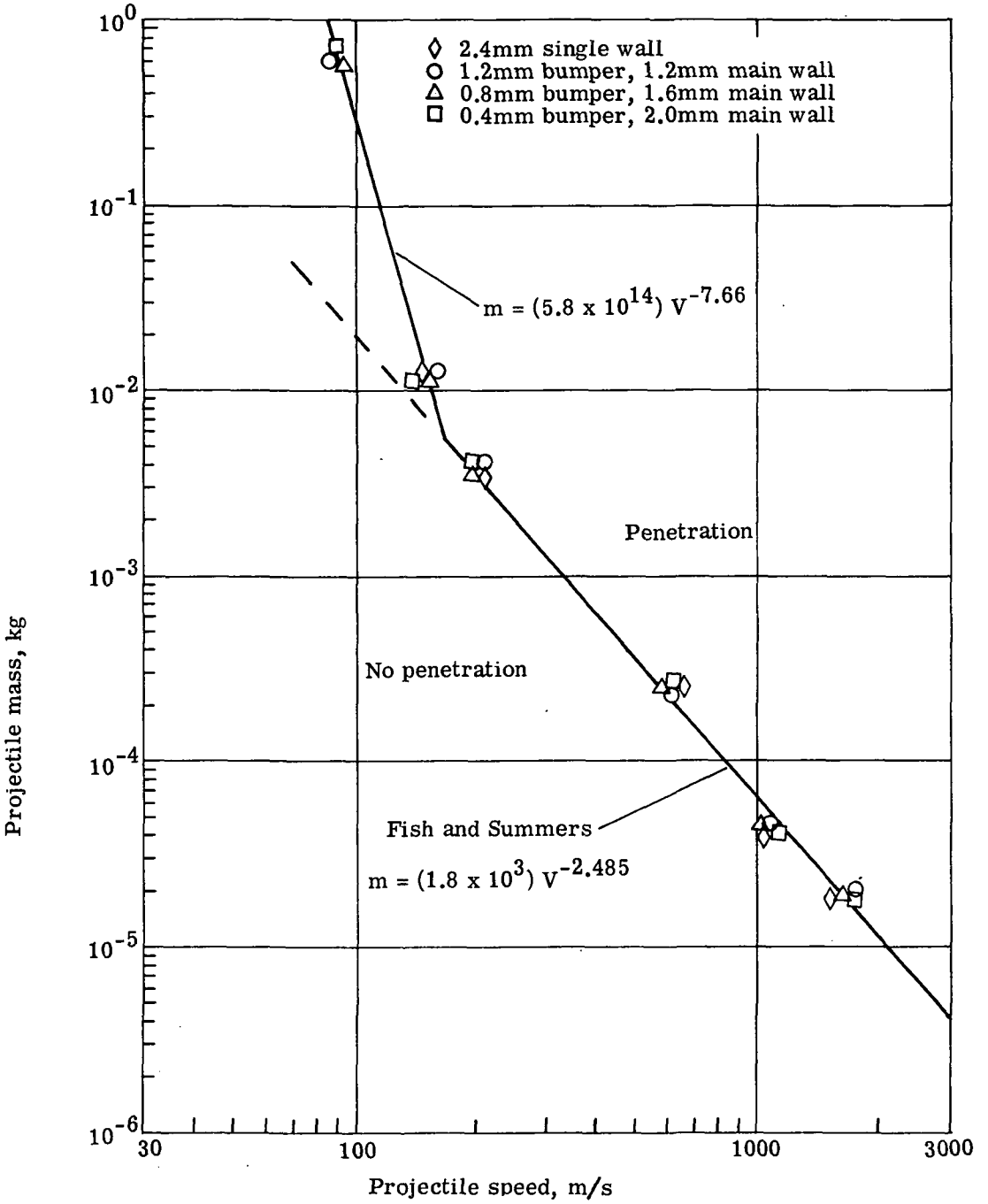

Figure 10.- Penetration resistance of aluminum structures to spherical aluminum projectiles. The impact angle was normal to the structure surface. The spacing was 25.4 mm for the double-wall structures.

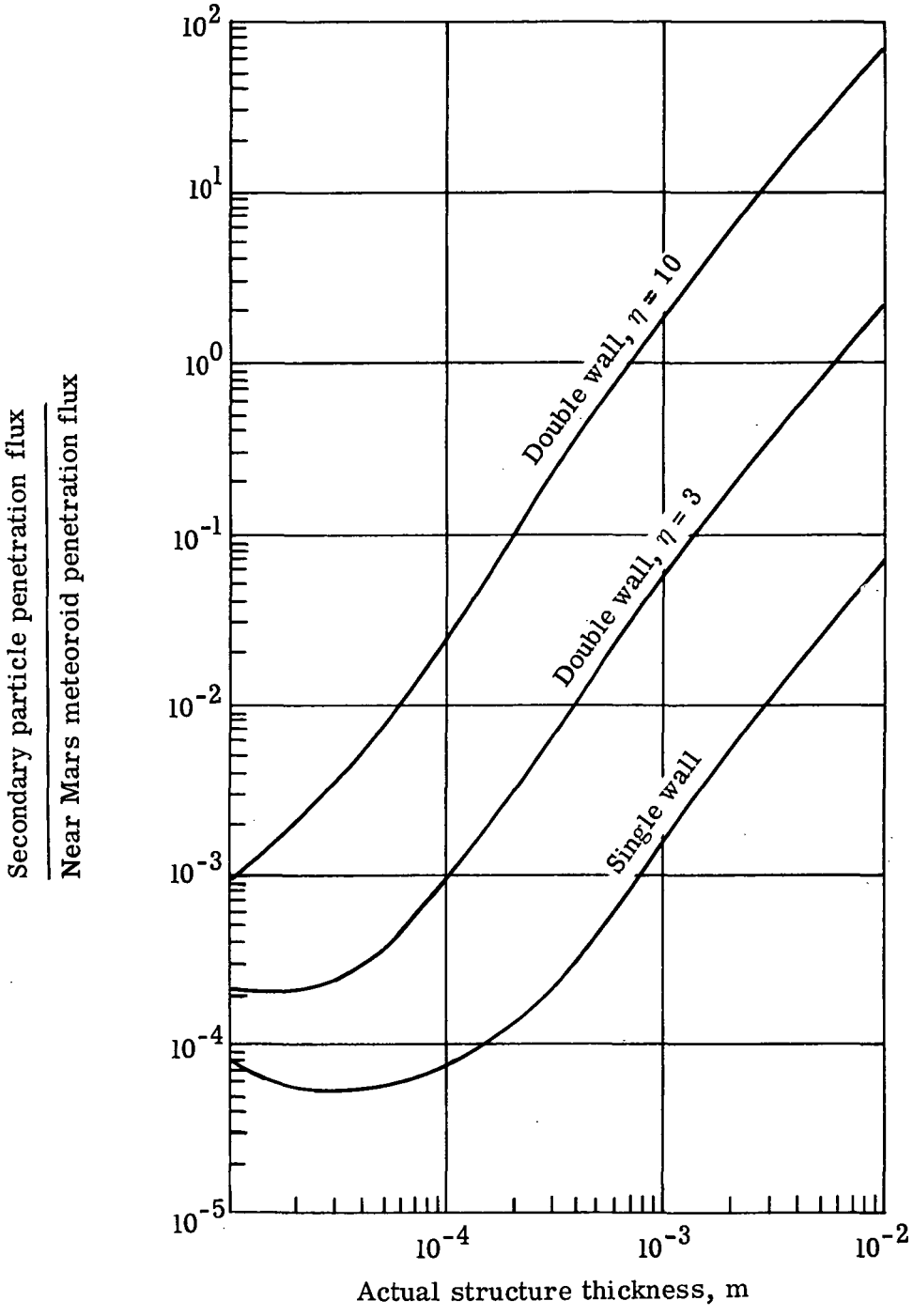

Figure 11.- Comparison of penetration flux from secondary particles and meteoroids through single-wall and double-wall aluminum structures. Secondary penetration flux is for structure on surface of Mars whereas meteoroid penetration flux is for structure outside of Martian atmosphere. η is the efficiency factor of double-wall structure against meteoroids.

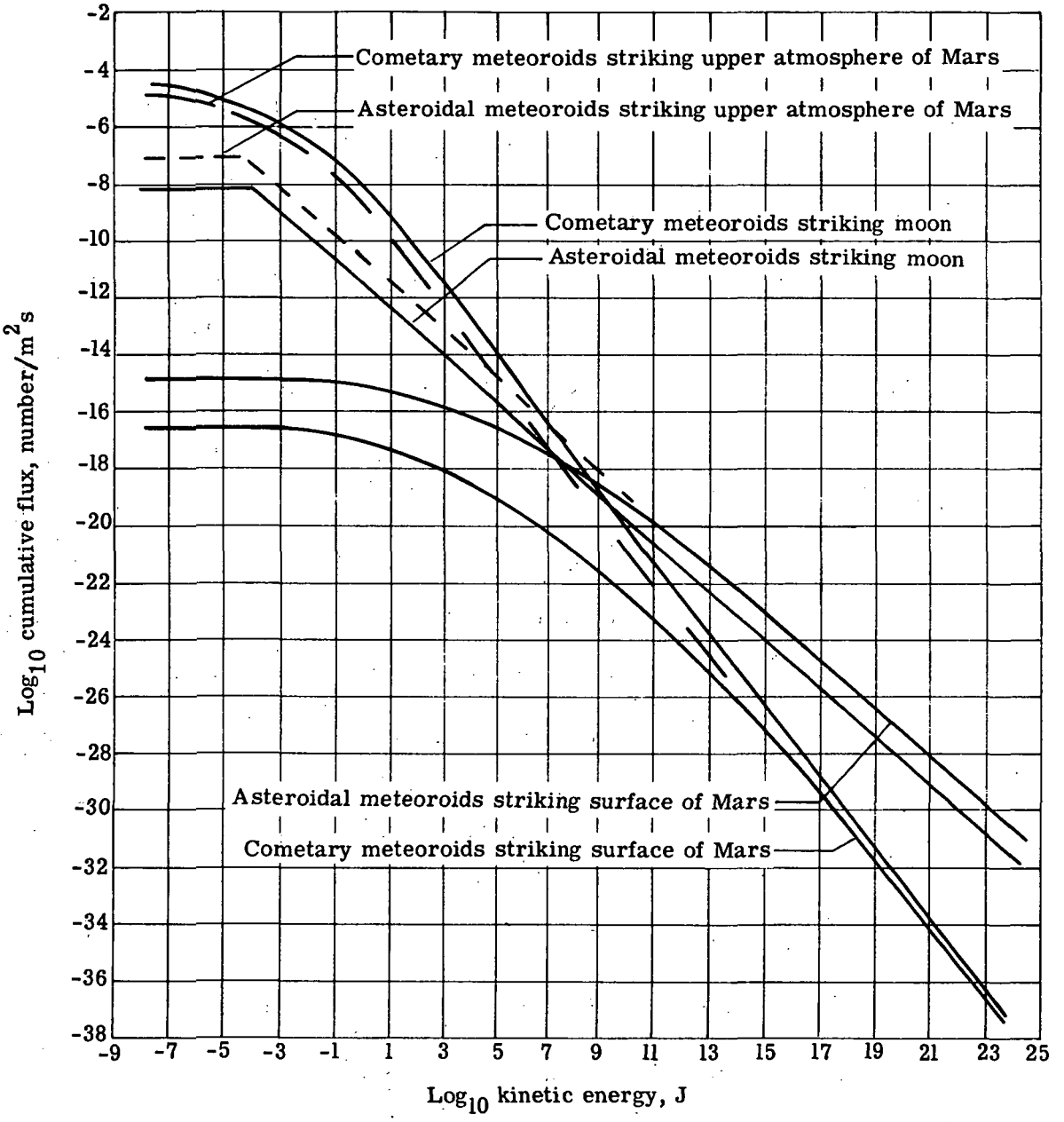

Figure 12.- Meteoroid flux on upper atmosphere and on surfaces of Mars and the moon.

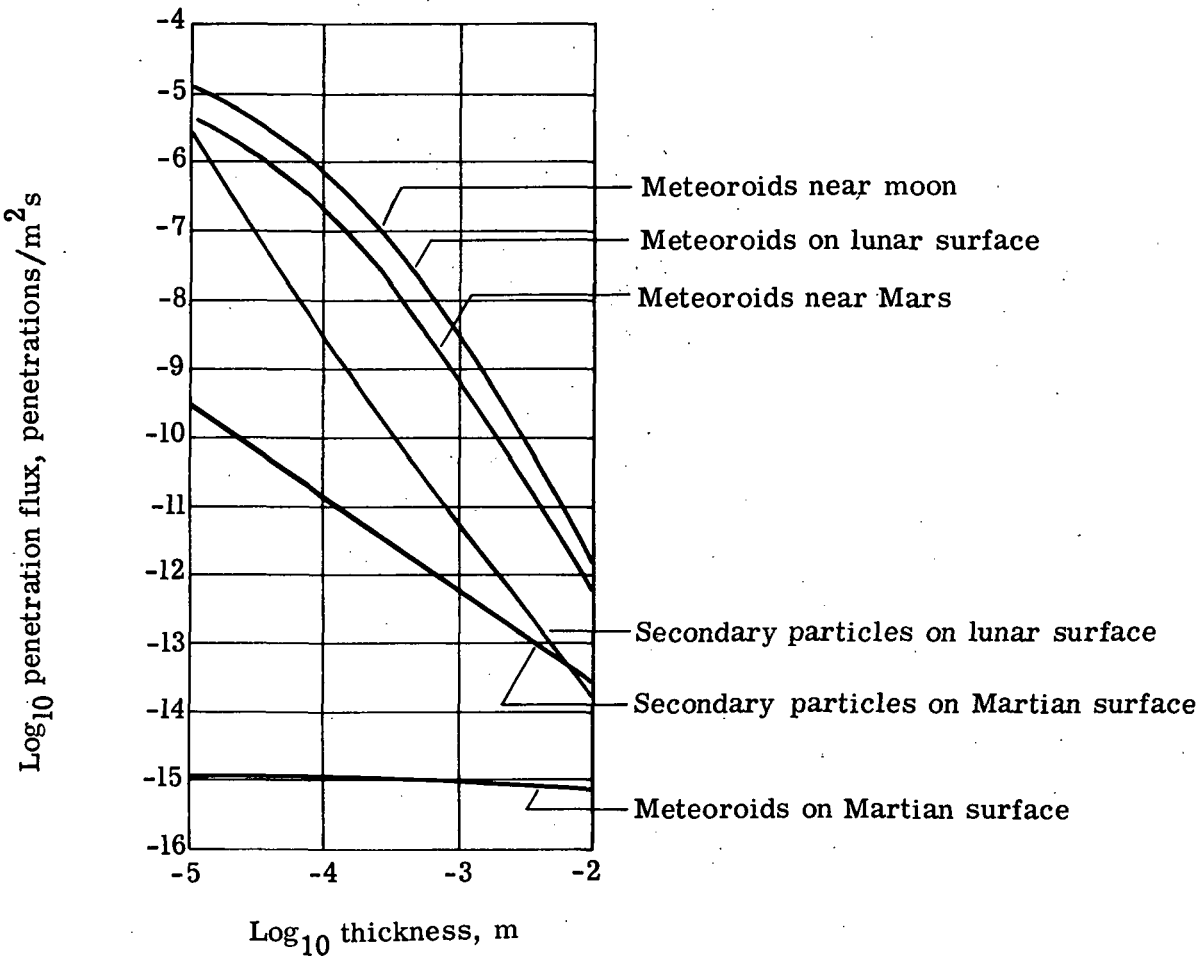

Figure 13.- Penetration flux for single aluminum plates in space near Mars, in space near the moon, on the surface of Mars, and on the surface of the Moon.

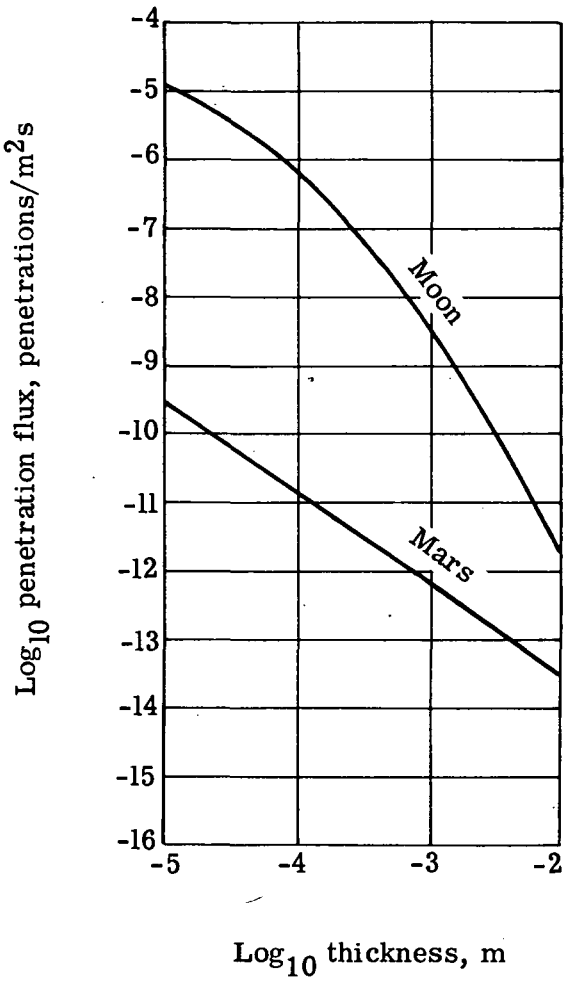

Figure 14.- Total penetration flux for single aluminum plates on the surface of Mars and the surface of the Moon. Total penetration flux includes penetration flux from meteoroids and from secondary particles.

NATIONAL AERONAUTICS AND SPACE ADMINISTRATION
WASHINGTON, D.C. 20546

OFFICIAL BUSINESS
PENALTY FOR PRIVATE USE $300

SPECIAL FOURTH-CLASS RATE BOOK

POSTAGE AND FEES PAID
NATIONAL AERONAUTICS AND SPACE ADMINISTRATION
451

U.S.MAIL

POSTMASTER: If Undeliverable (Section 158 Postal Manual) Do Not Return

"The aeronautical and space activities of the United States shall be conducted so as to contribute . . . to the expansion of human knowledge of phenomena in the atmosphere and space. The Administration shall provide for the widest practicable and appropriate dissemination of information concerning its activities and the results thereof."

—NATIONAL AERONAUTICS AND SPACE ACT OF 1958

NASA SCIENTIFIC AND TECHNICAL PUBLICATIONS

TECHNICAL REPORTS: Scientific and technical information considered important, complete, and a lasting contribution to existing knowledge.

TECHNICAL NOTES: Information less broad in scope but nevertheless of importance as a contribution to existing knowledge.

TECHNICAL MEMORANDUMS: Information receiving limited distribution because of preliminary data, security classification, or other reasons. Also includes conference proceedings with either limited or unlimited distribution.

CONTRACTOR REPORTS: Scientific and technical information generated under a NASA contract or grant and considered an important contribution to existing knowledge.

TECHNICAL TRANSLATIONS: Information published in a foreign language considered to merit NASA distribution in English.

SPECIAL PUBLICATIONS: Information derived from or of value to NASA activities. Publications include final reports of major projects, monographs, data compilations, handbooks, sourcebooks, and special bibliographies.

TECHNOLOGY UTILIZATION PUBLICATIONS: Information on technology used by NASA that may be of particular interest in commercial and other non-aerospace applications. Publications include Tech Briefs, Technology Utilization Reports and Technology Surveys.

Details on the availability of these publications may be obtained from:

SCIENTIFIC AND TECHNICAL INFORMATION OFFICE

NATIONAL AERONAUTICS AND SPACE ADMINISTRATION

Washington, D.C. 20546